nature plants

ARTICLES

PUBLISHED: 21 DECEMBER 2015 | ARTICLE NUMBER: 15196 | DOI: 10.1038/NPLANTS.2015.196

Blocking miR396 increases rice yield by shaping inflorescence architecture

Feng Gao[1†], Kun Wang[1†], Ying Liu[1], Yunping Chen[1], Pian Chen[1], Zhenying Shi[2], Jie Luo[3], Daqing Jiang[1], Fengfeng Fan[1], Yingguo Zhu[1] and Shaoqing Li[1*]

Strategies to increase rice productivity to meet the global demand have been the main concern of breeders around the world. Although a growing number of functional genes related to crop yield have been characterized, our understanding of its associated regulatory pathways is limited. Using rice as a model, we find that blocking miR396 greatly increases grain yield by modulating development of auxiliary branches and spikelets through direct induction of the growth regulating factor 6 (*OsGRF6*) gene. The upregulation of *OsGRF6* results in the coordinated activation of several immediate downstream biological clades, including auxin (IAA) biosynthesis, auxin response factors, and branch and spikelet development-related transcription factors. This study describes a conserved microRNA (miRNA)-dependent regulatory module that integrates inflorescence development, auxin biosynthesis and signalling pathways, and could potentially be used in engineering high-yield crop plants.

It is predicted that the world's population will reach 9 billion by 2050, which is highly likely to result in global food shortage. To cope with such a challenge, crop production needs to be doubled by 2050[1]. Rice plays a central role in safeguarding the security of global food supplies because over half of the world's population lives on it. Rice yield is largely determined by four factors: grain number, seed-setting rate, 1,000-grain weight and effective panicles per plant. Grain number has received the greatest attention due to its leading role in determining rice productivity[2]. Increasing evidence has revealed that grain number is governed by a series of factors that include transcription factors, plant hormones and microRNAs (miRNAs). These elements act as molecular switches that specify inflorescence architecture and size which in turn influence cereal yield[3].

miRNAs are a class of single-stranded small RNAs with lengths ranging from 21 to 24 nucleotides (nt) that regulate gene expression through transcriptional or translational inhibition[4–6]. It has been suggested that the expression of over one-third of protein-coding genes in eukaryotes is regulated by miRNAs[4]. Plant miRNAs have been shown to play a role in various processes including growth, development and stress resistance[4,7,8]. Disruption of the dynamic balance between miRNAs and their target genes may lead to drastic phenotypic changes[7].

Recently, miR156 and miR397 have been implicated in the control of rice yield. miR156 plays a critical role in the metabolic pathway that influences yield by regulating the expression of *OsSPL14* (*IPA1*)[9]. The accumulation of *IPA1* transcripts activates the expression of *TEOSINTE BRANCHED1* and *DENSE AND ERECT PANICLE1*[10], which in turn leads to the development of several additional axillary branch meristems from the axils, thereby resulting in larger inflorescence with dense branches and spikelets[11]. It has also been suggested that miR397 enhances rice yield by increasing spikelet number and grain size by suppressing laccase activity[12]. These findings elucidate the crucial roles of miRNAs in tailoring panicle pattern and rice yield, as well as determining the complexity of the regulatory network of yield. A number of yield-regulating genes such as *TAWAWA1* (ref. 13), *ABERRANT SPIKELET AND PANICLE1* (ref. 14), *ABERRANT PANICLE ORGANIZATION1* (ref. 15) and *LAX PANICLE1* (ref. 16) that are involved in the differentiation and initiation of the auxiliary branches of rice inflorescence have been genetically characterized. However, current knowledge regarding the roles of miRNAs in rice yield is limited; therefore, elucidating their functions in regulating panicle development and yield at the molecular level is warranted.

Hybrid rice generally has a ~20% higher yield than that of its parents, and this is mainly due to its significantly higher number of spikelets. Therefore, hybrid rice is an ideal model for studying the regulation of spikelet number. In rice, spikelet number is predominantly determined by inflorescence development. Recent studies have suggested that miRNAs play important roles in regulating of spikelet number[9,11,12]. To systematically identify the miRNAs regulating spikelet number, we compared the expression pattern of miRNAs in young inflorescences of the widely cultivated three-line hybrid, Yuetai-A/9311, and its parental lines (Supplementary Table 1) using miRNA microarray analysis. A total of 17 miRNAs showed significant differential expression patterns between hybrid F_1 and either of the parents (Yuetai-A and 9311; Supplementary Table 2), some of which were subsequently confirmed by RNA gel blotting and quantitative polymerase chain reaction with reverse transcription (qRT–PCR) analyses (Supplementary Fig. 1). To evaluate their functions, we constructed overexpression (OE) plasmids with 35S promoter for these miRNAs and transformed into *indica* rice Yuetai-B. Among these, the rice lines with overexpressed miR396b (OEmiR396b) showed phenotypic variations in inflorescence architecture. Seven out of ten OEmiR396b transgenic lines with elevated expression of miR396b (Supplementary Fig. 2a,c) displayed dwarf stature and abnormal inflorescence without the secondary branches and pedicels, and the spikelets were clustered together and sparsely scattered across the primary branches

[1]State Key Laboratory of Hybrid Rice, Key Laboratory for Research and Utilization of Heterosis in Indica Rice of Ministry of Agriculture, College of Life Science, Wuhan University, Wuhan 430072, China. [2]Institute of Plant Physiology & Ecology, SIBS, CAS. [3]National Key Laboratory of Genetic Crop Improvement, Huazhong Agriculture University, Wuhan 430070, China. †These authors contributed equally to this work. *e-mail: shaoqingli@whu.edu.cn

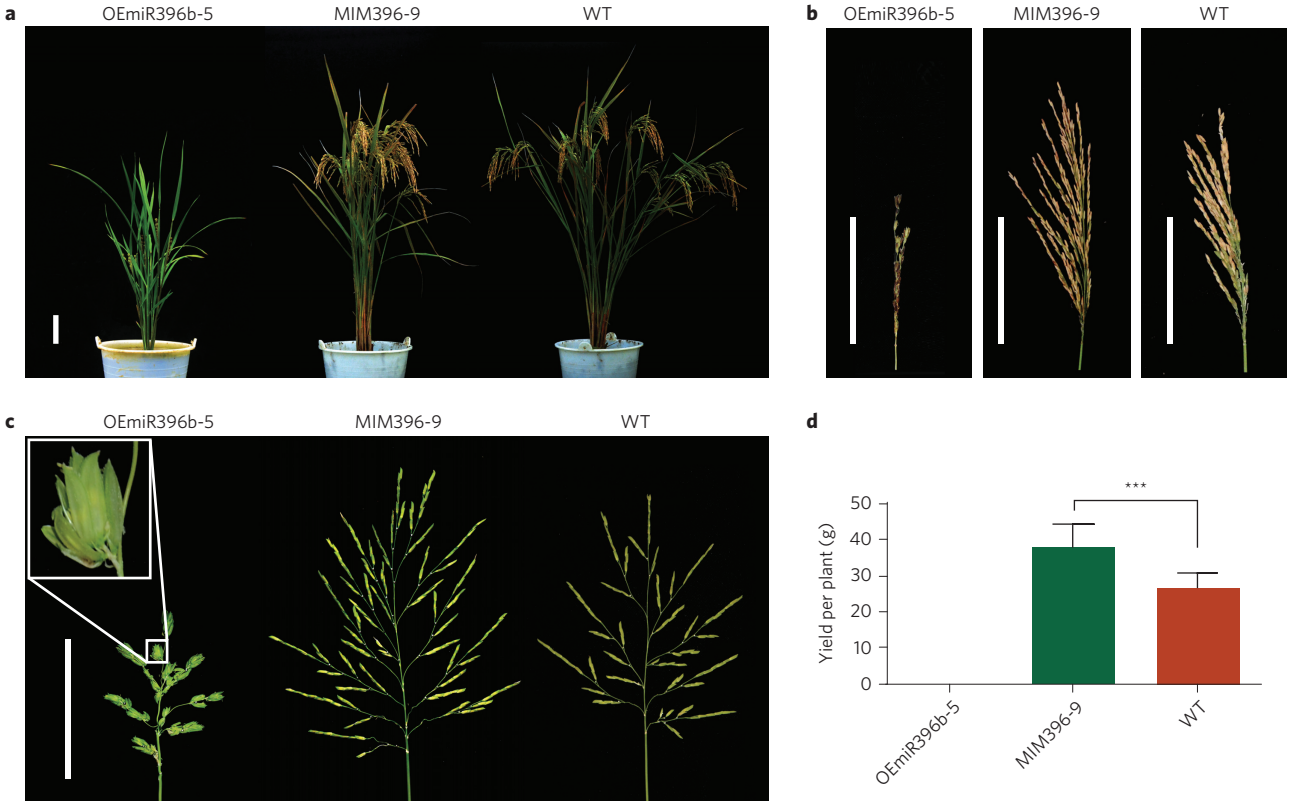

Figure 1 | Phenotypes of miR396b overexpression (OE) and miR396 mimicry (MIM) transgenic rice. a, Morphologies of gross plants. Scale bars, 10 cm. **b**, Mature panicles. Scale bars, 12 cm. **c**, Stretch young inflorescence. Magnification (left) highlights clustered spikelets. Scale bars, 12 cm. **d**, Grain yield per plant. Values are the means ± s.d., $n = 10$. Significant differences were calculated with Student's *t*-test, $^{***}P < 0.001$.

(Fig. 1). These results indicate that miR396b is a crucial factor in regulating inflorescence development, which was also consistent with the observation that the expression pattern of the miR396b precursor largely contributed to the expression of miR396 at the secondary branch stage, as shown by the results of qRT–PCR analysis (Supplementary Fig. 3)

To explore further the roles of miR396b, the target mimicry of miR396 (MIM396) was overexpressed in Yuetai-B to block miR396 activities. qRT–PCR analysis (Supplementary Fig. 2b,d), showed that 9 out of 12 MIM396 transgenic plants showed a significant increase in yield (41.8 ± 11.1%, $P < 0.001$) compared with that of the wild type (WT), which might have been due to the substantial increase in the number of secondary branches (56.4 ± 16.6%, $P < 0.001$) and spikelets (38.9 ± 12.6%, $P < 0.001$) (Fig. 1b,d and Supplementary Table 3). Together, these results demonstrate that miR396b controls rice inflorescence architecture and grain yield.

Plant miRNAs inhibit the expression of their target genes via base-pairing[4]. Previous studies have predicted that miR396 targets GRFs in plants[17–20]. The GRF transcription factor family comprises 12 members in rice, and the present study attempted to determine which of these were the crucial player(s) for rice inflorescence size and yield. Semi-quantitative PCR analysis revealed that *OsGRF6*, *OsGRF8*, and *OsGRF9*, which were grouped into the same subfamily in the phylogenetic tree (Supplementary Fig. 4a), were highly expressed at the early reproductive stage relative to the other members (Supplementary Fig. 4b), which suggests that these three genes might possibly be the regulator(s) of inflorescence development. We therefore were prompted to identify which one(s) were responsible for the establishment of inflorescence architecture and the determination of spikelet number. Overexpression constructs of *OsGRF6*, *OsGRF8* and *OsGRF9* that were driven by the 35S promoter were individually transformed into the WT. The yield of the OEGRF6 transgenic lines increased by 47.6 ± 15.7% ($P < 0.001$) compared with that of the WT, whereas a slight increase was observed in the OEGRF8 (8.0 ± 3.8%, $P > 0.05$) and OEGRF9 (6.8 ± 4.7%, $P > 0.05$) lines (Fig. 2a,e). In OEGRF6-1, a line of OEGRF6, the number of primary branches, secondary branches and spikelets increased by 23.0 ± 6.1% ($0.01 < P < 0.05$), 59.3 ± 12.9% ($P < 0.001$), and 54.3 ± 9.1% ($P < 0.001$), respectively (Fig. 2b–d). No significant differences in growth period, plant height and effective panicle between OEGRF6 and WT were observed (Supplementary Fig. 5f–h). Similar to the OEmiR396b lines, *OsGRF6* interference (GRF6-RNAi) rice (Supplementary Fig. 6a) showed dwarfism, a lower number of panicles, abnormal inflorescence with shrunken panicles and no secondary branches (Fig. 3a and Supplementary Fig. 6b). Thus, we concluded that *OsGRF6* promotes the development of inflorescence and spikelet number in rice.

To validate further the relationship between spikelet number and the miR396b/*OsGRF6* regulation pathway, we generated a miR396-resistant version of *OsGRF6* (OErGRF6, Supplementary Fig. 7a) transgenic rice. As expected, the expression levels of *OsGRF6* increased in OErGRF6 lines (Fig. 3b and Supplementary Fig. 6c), and the OErGRF6 lines showed an increase in the number of secondary branches and spikelets, as well as a higher yield than that observed in the WT (Fig. 3c and Table 1). These results demonstrated that expression of *OsGRF6* was directly regulated by miR396b.

The MIM396 and OEGRF6 transgenic plants showed high yield relative to that of the WT at the individual level. To determine whether this holds true in field tests, the transgenic lines MIM396-9, OEGRF6-1 and OErGRF6-2 and WT rice were tested in two experimental sites. Compared with the WT, the yield of MIM396-9, OEGRF6-1 and OErGRF6-2 plants increased by

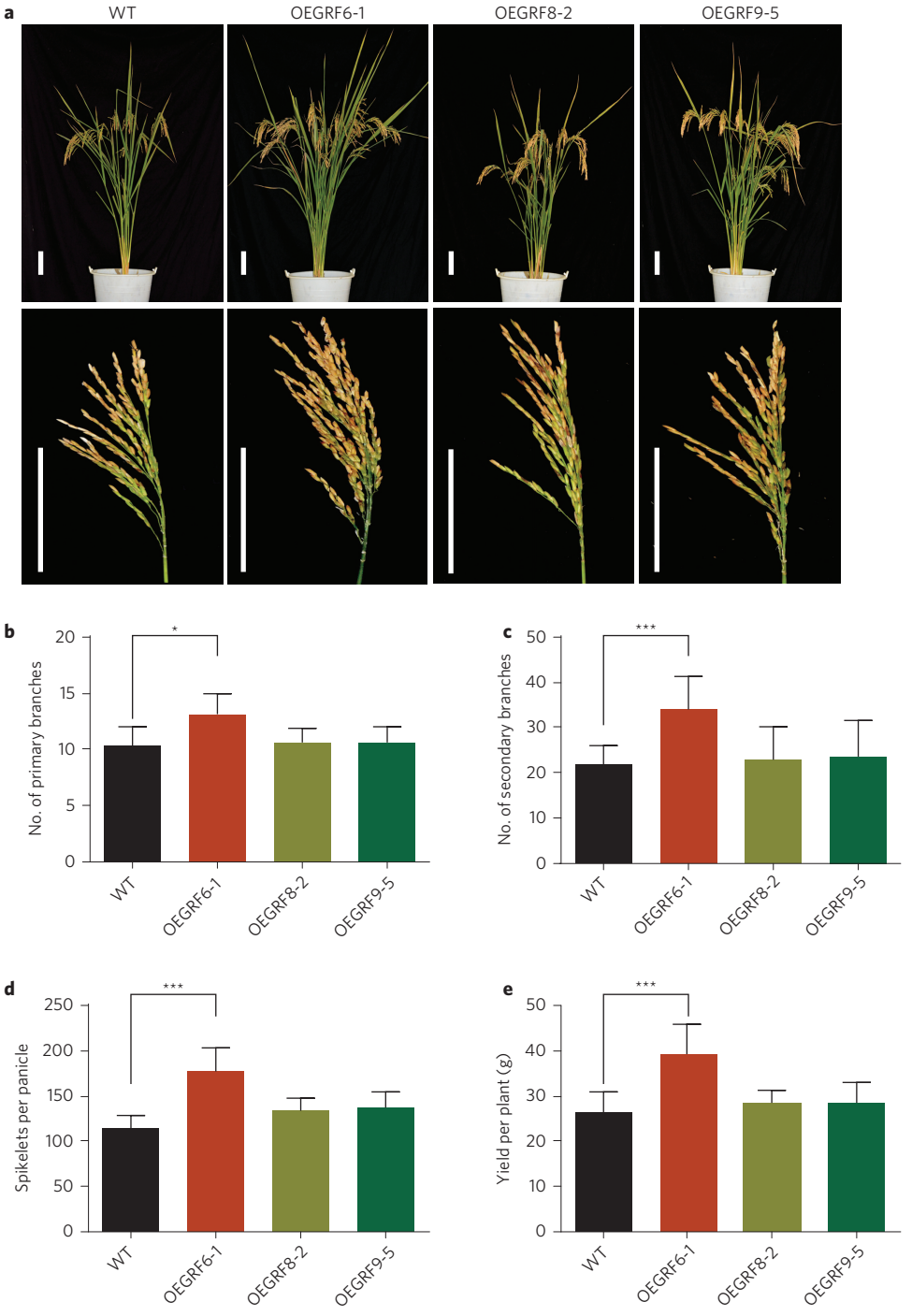

Figure 2 | Phenotypes and agronomic traits of *OsGRF6*, *OsGRF8* and *OsGRF9* overexpression (OE) transgenic plants. a, Gross plant (upper panel) and panicle (lower panel) morphologies of rice. Scale bars, 12 cm. **b**, Number of the primary branches per panicle of rice ($n = 30$). Values are the means ± s.d., $^{*}P < 0.05$. **c**, Number of the secondary branches per panicle of rice ($n = 30$). Values are the means ± s.d., $^{***}P < 0.001$. **d**, Spikelets per panicle of rice ($n = 30$). Values are the means ± s.d., $^{***}P < 0.001$. **e**, Yield per plant of rice ($n = 10$). Values are the means ± s.d., $^{***}P < 0.001$.

16.8%, 18.1% and 10.4% in Wuhan and 15.4%, 16.0%, and 17.3% in Hainan, respectively (Table 1). These observations were in line with the results at the individual level, suggesting that expression of miR396 targets mimicry or its target gene *OsGRF6* significantly increased yield at the population level. Furthermore, we investigated yield-related components to determine which agronomic characters largely contributed to the observed yield increase in the transgenic lines. The 1,000-grain weight and seed-setting rate showed no apparent changes between transgenic lines and WT. However, the spikelet number of the MIM396-9, OEGRF6-1 and OErGRF6-2 plants significantly increased relative to that of the WT (Table 1). These results further confirmed that at the population level, the MIM396 and OEGRF6 transgenic plants showed a significant improvement in rice yield by increasing spikelet number.

To determine how miR396b regulates *OsGRF6* expression, the spatiotemporal distribution of miR396b and *OsGRF6* was investigated. qRT–PCR analysis showed that miR396b and *OsGRF6* exhibited anti-correlated expression patterns (Supplementary Fig. 8),

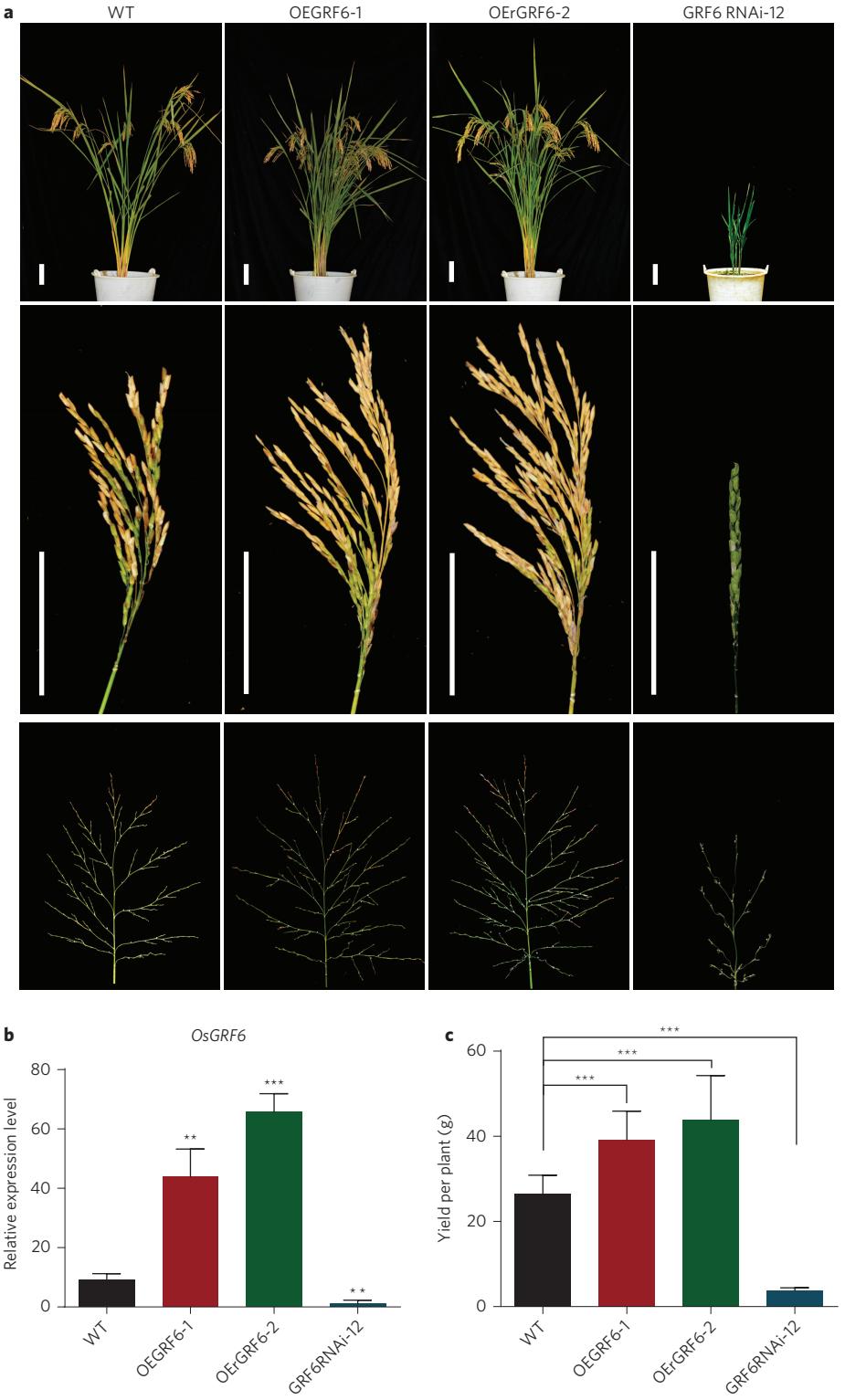

Figure 3 | | Plant phenotypes and grain yield of *OsGRF6* associated transgenic rice lines. a, Morphologies of the gross plants (upper panel), panicles (middle panel) and pedicel (lower panel) of WT, *OsGRF6* overexpression (OEGRF6-1 and OErGRF6-2) and GRF6 RNAi-12 transgenic plants. Scale bars, 12 cm. **b**, RNA expression level of *OsGRF6* of the corresponding transgenic rice. Values are expressed as the means ± s.d., $n = 3$. $^{**}P < 0.05$, $^{***}P < 0.001$. **c**, Yield per plant of the corresponding transgenic rice. Values are expressed as the means ± s.d., $n = 10$. $^{***}P < 0.001$.

thereby indicating that *OsGRF6* expression was highly dependent on the level of miR396b *in vivo*. To confirm this finding, we performed RNA *in situ* hybridization of miR396 and *OsGRF6* using the inflorescence meristem of MIM396-9, OEmiR396b-5 and WT plants. As expected, the expression levels of miR396 followed a decreasing order: OEmiR396b-5 > WT > MIM396-9 in the secondary primordium, whereas the expression level of *OsGRF6* in the same three plants followed the opposite order (Supplementary Fig. 9). These investigations were in line with the results of RNA ligase-mediated rapid amplification of cDNA ends (RLM-RACE) analysis in that

Table 1 | Grain yield and associated components in transgenic rice in field trials.

Sites	Characters	WT	MIM396-9	OEGRF6-1	OErGRF6-2
Wuhan	Effective panicle	9.2 ± 2.0	11.5 ± 2.3	10.9 ± 2.2	11.7 ± 2.6
	Spikelet number	144.8 ± 20.6	184.6 ± 20.5**	180.3 ± 24.1**	184.1 ± 17.9**
	Seed-setting rate (%)	63.8 ± 2.3	60.9 ± 3.6	62.1 ± 2.5	61.9 ± 2.9
	1,000-grain weight (g)	22.12 ± 0.1	22.07 ± 0.1	22.05 ± 0.1	22.06 ± 0.1
	Grain yield (kg per plot)	5.35 ± 0.12	6.26 ± 0.27**	6.34 ± 0.34**	5.93 ± 0.13*
	Yield increase (%)	-	16.8 ± 0.2	18.1 ± 0.2	10.4 ± 0.2
Hainan	Effective panicle	9.6 ± 1.9	10.7 ± 2.1	10.8 ± 1.8	11.1 ± 2.0
	Spikelet number	138.6 ± 19.7	185.2 ± 22.1**	184.1 ± 18.8**	184.9 ± 21.5**
	Seed-setting rate (%)	86.9 ± 2.3	80.7 ± 2.8	82.2 ± 1.9	82.7 ± 2.0
	1,000-grain weight (g)	22.14 ± 0.1	22.13 ± 0.1	22.12 ± 0.1	22.14 ± 0.1
	Grain yield (kg per plot)	7.29 ± 0.16	8.41 ± 0.18**	8.46 ± 0.19**	8.55 ± 0.22**
	Yield increase (%)	-	15.4 ± 0.2	16.0 ± 0.2	17.3 ± 0.2

Values shown are the means ± s.d. ($n = 3$ for grain yield, $n = 30$ for the rest). *$P < 0.05$, **$P < 0.01$.

OsGRF6 mRNAs were spliced between the 11th and 12th bases of the miR396b target region (Supplementary Fig. 7b).

Rice inflorescence architecture is determined by the initiation of the primordia as well as the occurrence and elongation of the primary and the secondary branches and spikelets[21]. To confirm the role of miR396b and *OsGRF6* in the development of secondary branches, scanning electron microscopy (SEM) was performed. The secondary branch primordia of OEmiR396b lines were barely differentiated from the primary branches, and the inflorescences showed extensive collapse at the the later of spikelet primordia stage (Supplementary Fig. 10). These results were indicative of the arrest of outgrowth and elongation of the auxiliary branches and spikelets. In contrast, both MIM396 and OEGRF6 plants showed a higher number of primary branch primordia and secondary branch primordia than that in the WT. Together, our results indicated that the miR396b-*OsGRF6* module plays a critical role in controlling the development of secondary branches in rice inflorescences.

To understand how *OsGRF6* regulates rice inflorescence architecture, we employed chromatin immunoprecipitation followed by sequencing (ChIP-seq) to map *OsGRF6* target genes at the genome-wide level. The *p35S:GRF6–GFP* (green fluorescent protein) transgenic line, which exhibits a similar phenotype to that of *GRF6*-overexpressing lines, was used in the present study. Because of limitation of available young inflorescences at the secondary branch initiation stage, the calli of *p35S:GRF6–GFP* transgenic lines were used as alternative. DNA precipitated by using an anti-GFP antibody and input DNA (genomic DNA before immunoprecipitation) were subjected to high-throughput sequencing and designated as 'GRF6' and 'Input', respectively. Statistically significant binding peaks were defined by comparing the parallel 'GRF6' and 'Input' using the MACS algorithm[22]. Based on the sequences of a total of 200 peaks mapped onto the rice genome (Supplementary Fig. 11 and Supplementary Table 6), an OsGRF6-binding motif 'CGSMR' ($e = 5.5 \times 10^{-21}$) was predicted (Fig. 4a), which was validated by electrophoretic mobility shift assay (EMSA) (Fig. 4c).

To determine which genes were regulated by MIM396/OsGRF6 signals during the development of inflorescence, the transcriptomes of MIM396-9 and WT in young inflorescences at the secondary branch primordial stage were compared using RNA-seq. A total of 329 up- and 568 downregulated (ratio ≥ 2 or ≤ 0.5, and false discovery rate (FDR) < 0.05) genes were detected in the MIM396-9 plants (Supplementary Data 2). Of which, *OsTAWAWA1* (LOC_Os10g33780) and *OsMADS34* (LOC_Os03g54170), two essential inflorescence development-related genes, showed significantly higher expressions levels in the MIM396-9 line (Supplementary Table 4 and Supplementary Fig. 12), which indicated that OsGRF might activate the expression of these two genes. Although, no binding peaks of OsGRF6 were found in the promoters of the two genes based on ChIP-seq in calli tissue, their promoters had enriched 'CGSMR' motifs and could be bound by the glutathione *S*-transferase (GST)–OsGRF6 protein *in vitro*, as indicated in the EMSA assays (Supplementary Fig. 13c,d). These findings corroborate the roles of *OsTAWAWA1* in controlling spikelet number and rice grain yield[13], and that *OsMADS34* modulates not only the auxiliary branches of inflorescences, but also spikelet number and morphology[23].

Next, the biological significance of the differentially expressed genes in the RNA-seq data was determined by performing enrichment analyses of gene ontology categories (Supplementary Data 3) using DAVID tools[24]. Significantly enriched upregulated genes were mainly involved in auxin synthesis and auxin signal response (*YUCCA*, *ARFs* and *GH3*), as well as in a series of biological processes related to auxin response such as cell division (mitosis phase), cytoskeleton, cell wall organization and response to light stimulus[25]. In ChIP-PCR analysis (Fig. 4e), auxin biosynthesis-related *OsYUCCA-like* (*FMO*)[26] and auxin response factors *OsARF2* and *OsARF7*, displayed OsGRF6-binding peaks (Fig. 4d). Consistent with the observed increased expression of *OsYUCCA-like*, *OsARF2* and *OsARF7*, expression of *OsYUCCA1* and *OsARF11* was significantly upregulated in the inflorescence of the MIM396-9 line, indicating that these may also be the direct targets of the OsGRF6, as revealed by the results of EMSA assays (Supplementary Fig. 13a,b). These finding suggest that OsGRF6 could possibly be involved in the synthesis of active auxin (IAA), as well as in the auxin signalling pathway. Supporting this finding is the observation that the IAA content of the MIM396 young inflorescences was significantly higher than that of the OEmiR396b and WT (Supplementary Fig. 14). Taken together, these finding indicate that OsGRF6 is a positive player of IAA biosynthesis and the signalling pathway, which are both involved in early inflorescence development.

Three sequential developmental processes, namely the primary branch, the secondary branch and spikelet speciation, dynamically establish rice inflorescence architecture[21]. The former rachis branch meristem becomes the determinant of the next order lateral meristems that will eventually acquire the spikelet identity and terminates[27]. Coordinated cell differentiation, patterning and growth of inflorescence primordia spatiotemporally regulate the spikelet meristem fate of grass inflorescences, and subsequently, the grain number per panicle[21]. Recently, significant progress has been made towards understanding the molecular mechanism underlying the regulation of rice inflorescence architecture. Over 50 conserved genes have been determined to be involved in these complex processes in rice and other plants[28]. A few of these are regulated by miRNAs such as miR156 (ref. 9) and miR397 (ref. 12), which form independent regulatory circuits of yield control by modulating grain number or grain size in crops.

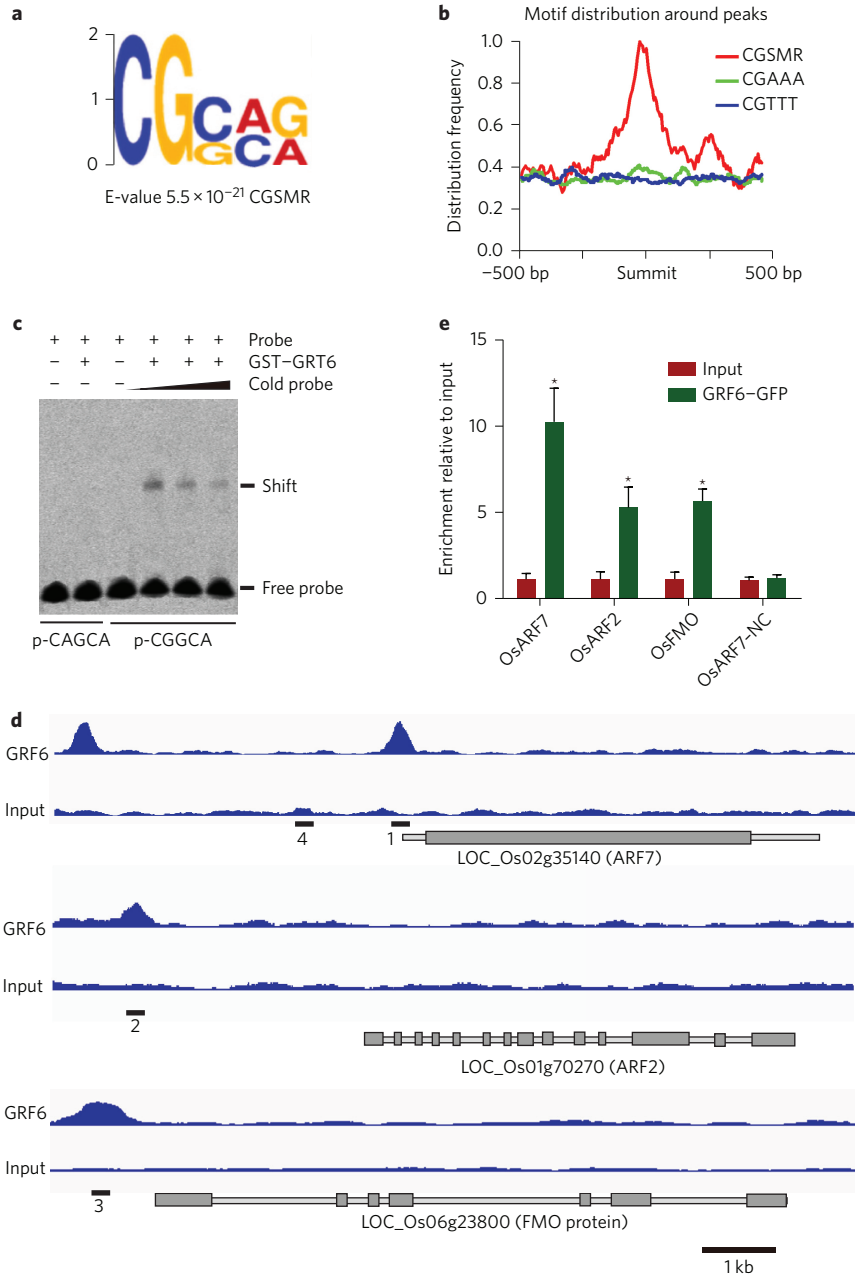

Figure 4 | CHIP-seq analysis of the OsGRF6 protein-bound *cis*-element and promoters of related genes. a, Putative GRF6-binding motifs predicted by DREME (see Methods). **b**, Motif distribution frequency within ± 500 bp of peak summits. **c**, EMSA validation of binding between OsGRF6 and motif 'CGGCA' (CGSMR). 'CAGCA' was used as control. **d**, Visualization of OsGRF6 binding peaks in the promoters of *OsARF7*, *OsARF2* and *OsYUCCA-like*. Black lines indicate probe locations (1–3, *OsARF7 OsARF2*, *OsYUCCA*; 4, *OsARF7*-NC, as negative control). **e**, ChIP-PCR validation for the binding sites on promoters. Values are expressed as the means of triplicates ± s.d.

The present study has determined that miR396b-*OsGRF6* regulates rice yield by coordinately modulating the expression of *YUCCA1*, *ARF2*, *ARF7*, *ARF11*, *OsTAWAWA1* and *OsMADS34* (Supplementary Figs 12 and 13). Among these, *OsTAWAWA1* and *OsMADS34* have been verified as crucial components of inflorescence development by activating the expression of downstream genes[13,23]. Moreover, *OsYUCCA1*, *OsARF2*, *OsARF7* and *OsARF11* have been determined to participate in the biosynthesis and signalling pathway of auxin[29–31]. It is well documented that AUX/IAA plays a central role in cell differentiation, organ formation and morphogenesis of plants[30]. The high level of expression of these auxin pathway-related genes in the primordia of the secondary branch (Supplementary Data 1 and 2) implies that AUX/IAA plays an important role in rice inflorescence development or determination. The direct regulation of *OsYUCCA1* and *OsARFs* by OsGRF6 (Fig. 4) reveals that miR396b-*OsGRF6* acts as a key component that defines the relationship among auxin biosynthesis, signalling pathway and inflorescence architecture to control rice grain number (Fig. 5). This present study clearly shows the direct relationship between miRNA and auxin signalling in rice inflorescence organ patterning.

The miR396b-*OsGRF6* module might regulate inflorescence architecture in a distinct pathway that is different from that of miR156 and miR397. OsGRF6 intricately balances the expression between *OsTAWAWA1* and *OsMADS34* (Supplementary Table 4), auxin synthesis and signalling proteins in MIM396 transgenic plants (Supplementary Figs 12 and 13). The orchestrated expression

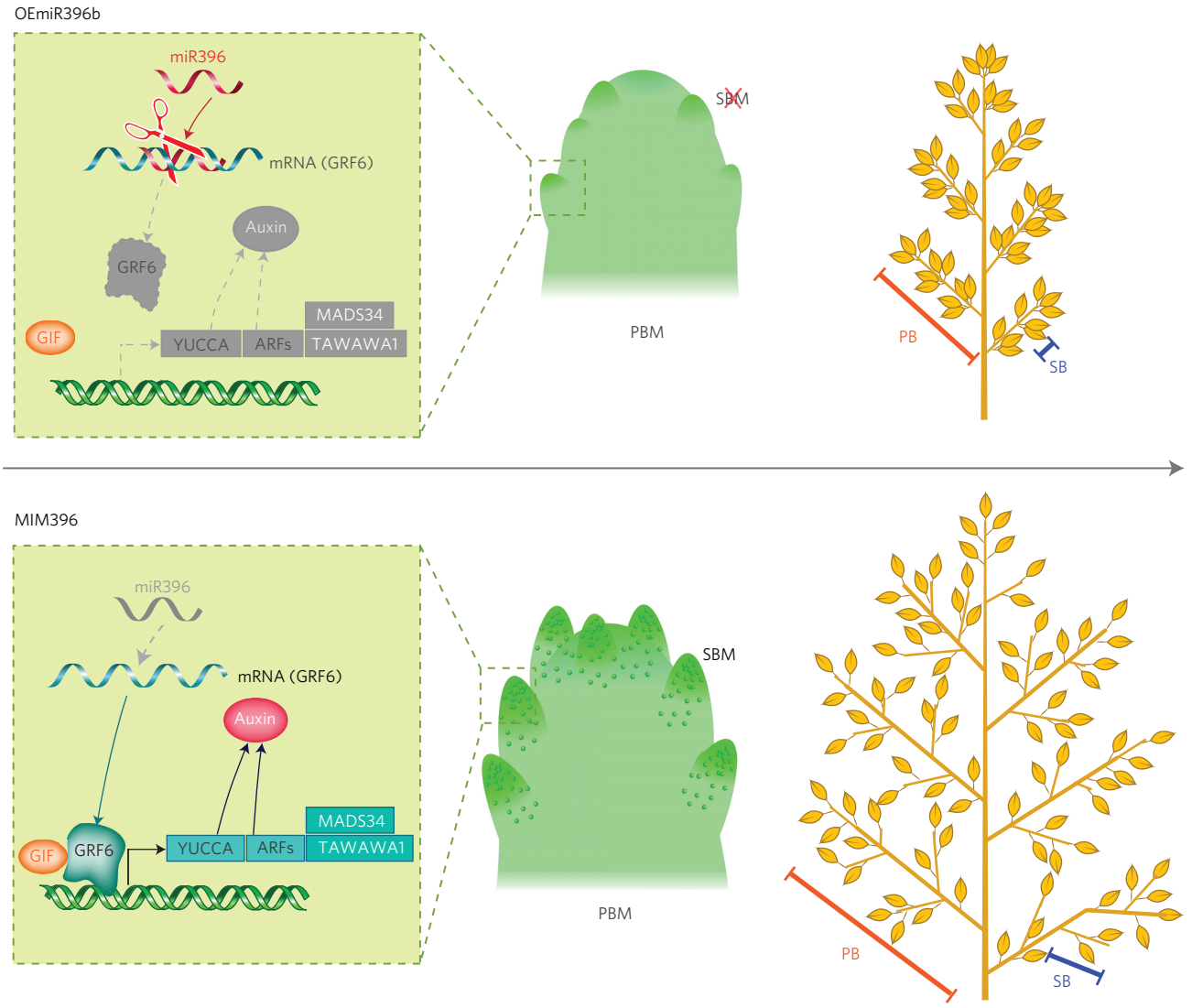

Figure 5 | A model of the miR396b-GRF6 module for the regulation of rice grain yield. In OEmiR396b plants, miR396b cleaved the *OsGRF6* transcripts to repress OsGRF6 expression and the downstream pathway for SBP development that was activated by OsGRF6. On the other hand, in MIM396 plants, the transcription factor OsGRF6 upregulated the expression of *OsMADS34* and *OsTAWAWA1*, and enhanced auxin synthesis, whereas the response genes (*OsYUCCA* and *OsARFs*) promoted SBP initiation and axis elongation. PB, primary branch; SB, secondary branch; PBP, primary branch primordia; SBP, secondary branch primordia.

of these factors promotes the branching of inflorescence, which in turn results in an increase in rice yield (Table 1). As miR396 and GRF are highly conserved in different crops[17–20,32,33], the results of the present study has shown that the miR396b-*OsGRF6* module might have been conserved to regulate inflorescence architecture, which could be utilized in developing molecular breeding strategies for the improvement of crops at the miRNA level.

Methods

Plant materials. Rice Yuetai-B (*Oryza sativa* L. ssp. indica) was used in the experiments. The control and transgenic plants were grown in the experimental field of Wuhan University, and field tests were performed in Huashan town (Wuhan, China) and Lingshui (Hainan, China) during summer with normal daily management.

Generation of transgenic rice plants. The 1 kb genomic DNA region flanking pri-miR396b and the cDNAs of *OsGRF6*, *OsGRF8* and *OsGRF9* were cloned into the pH7WG2D plasmid (ref. 34) to produce overexpression plants. The vector pANIC 8A (TAIR, http://www.arabidopsis.org/) was used for *OsGRF6* RNAi. rGRF6 was generated by two rounds of mutagenic PCR. The miR396b target mimicry vector was constructed as described elsewhere[35]. *Agrobacterium*-mediated transformation[36] was used in generating transgenic plants (Supplementary Table 5).

Agronomic trait observation and field test. The agronomic characters were investigated at the mature stage. Five to ten individual plants from each sample were subjected to statistical analysis. For the yield test, T_2 transgenic and WT plants were grown in the field under natural conditions. The plot area was 360 × 180 cm^2, with ten plants in each line and 20 plants in each column.

Real-time qPCR. Real-time qPCR experiments were independently performed in triplicate using the SYBR Green PCR Master Mixture (Roche, Germany). ChIP-qPCR was performed using the input and IP DNA from three biological replicates. The primers for the *OsGRF6* binding peaks and non-peak regions (based on ChIP-seq data) were designed as positive and negative controls. Fold enrichment was calculated against the promoter of the *Ubiquitin* gene. All the primers used in the study are listed in Supplementary Table 6.

Small RNA gel blotting and 5′ RACE. Approximately 35 μg of total RNA was separated in a 17% polyacrylamide gel with 7 M urea denaturing gels, transferred to a Hybond-N+ membrane (Roche) and then hybridized with digoxigenin-labelled locked nuclear acid (LNA) DNA probes (EXIQON). Detection was performed with anti-digoxigenin-AP and CDP-Star (Roche). 5′ RACE was performed with the GeneRace kit (Invitrogene).

Scanning electron microscopy and *in situ* hybridization. Fresh young panicles were fixed in 4% paraformaldehyde for 2 h, then dehydrated through an ethanol series ranging from 15~100%. The samples were dried to critical point and mounted

on stubs, and then examined under a scanning electron microscope (Hitachi S-3000N, Japan). For *in situ* hybridization[37], young panicles fixed in 4% paraformaldehyde were embedded in paraplast, from which 7 μm sections were prepared and then hybridized with miR396 and *OsGRF6* probes. Hybridization signals were detected with anti-digoxigenin-AP and NBT/BCIP (Roche).

RNA-seq and data analysis. Young inflorescences from each plant sample were collected for total RNA extraction. Library construction was performed with a NEBNext Multiplex RNA Library Prep Set for Illumina (NEB) and sequenced on an Illumina Hiseq2000 Platform. The clean reads were mapped to the rice genome[38] (version 7.0) using Cufflink (http://cufflinks.cbcb.umd.edu/). For gene expression analysis, the number of fragments per kilobase of exon per million fragments (FPKM) was calculated. The differentially expressed genes were defined as that fulfilling the following requirement: FDR ≤ 0.05 and ratio ≥ 2 or ≤ 0.5. DAVID[24] was used for the analysis of over-representation of gene classes.

ChIP-seq analysis. ChIP assays were conducted in p35S:GRF6–GFP transgenic lines as described elsewhere[39]. Polyclonal anti-GFP antibodies (Abcam AB290) were used in IP. The DNA samples from the precipitation and input were constructed into sequencing libraries using the Kapa Hyper Prep Kit (KAPABIOSYSTEMS) and sequenced by using the Hiseq 2000 system. Clean reads were mapped to the rice genome[38] using Bowtie[40]. Binding peaks were obtained by conducting MACS (ref. 41), with a p-value cutoff of 10^{-5}. The reads per million (RPM) around the peak summit (± 5 kb) was documented with a 100-nt window size to calculate the average enrichment level of the peak. To predict binding motifs, the flanking sequences of all peak summits (± 50 bp) were filtered by RepeatMasker (http://www.repeatmasker.org) and then analysed with DREME (ref. 42). Motif distribution frequency within the peak summit ± 500 bp was calculated using a 50-nt window size.

Electrophoretic mobility shift assay. The GST–GRF6 was expressed in *E. coli* BL21 cells with pGEX 6p-1 and then purified. Fluorescence probes were prepared by PCR using 5′-FAM labelled primers. The signals were scanned by typhoon 2,000 (GE Healthcare)[43,44].

Phytohormone measurement. Auxin (IAA) content was quantified by using liquid chromatography mass spectrometry (LCMS) as previously reported[45]. Fresh inflorescences were collected and ground into powder using liquid nitrogen. Approximately 100 ± 5 mg of powder was extracted using 1.5 ml of methanol. The supernatant was lyophilized in a freeze-drier (Thermo SAVANT SC110A-230) and then resuspended in 85% (v/v) methanol in water for LCMS analysis.

Accession numbers. High-throughput sequencing data analysed in the present study are available in the Gene Expression Omnibus under accession number GSE72694.

Received 10 August 2015; accepted 03 November 2015; published online 21 December 2015

References

1. McClung, C. R. Making hunger yield. *Science* **344,** 699–700 (2014).
2. Xing, Y. & Zhang, Q. Genetic and molecular bases of rice yield. *Annu. Rev. Plant Biol.* **61,** 421–442 (2010).
3. Sreenivasulu, N. & Schnurbusch, T. A genetic playground for enhancing grain number in cereals. *Trends Plant Sci.* **17,** 91–101 (2012).
4. Jones-Rhoades, M. W., Bartel, D. P. & Bartel, B. MicroRNAs and their regulatory roles in plants. *Annu. Rev. Plant Biol.* **57,** 19–53 (2006).
5. He, L. & Hannon, G. J. MicroRNAs: small RNAs with a big role in gene regulation. *Nature Rev. Genet.* **5,** 522–531 (2004).
6. Chen, X. A microRNA as a translational repressor of APETALA2 in *Arabidopsis* flower development. *Science* **303,** 2022–2025 (2004).
7. Mallory, A. C. & Vaucheret, H. Functions of microRNAs and related small RNAs in plants. *Nature Genet.* **38,** S31–S36 (2006).
8. Navarro, L. *et al.* A plant miRNA contributes to antibacterial resistance by repressing auxin signaling. *Science* **312,** 436–439 (2006).
9. Jiao, Y. *et al.* Regulation of *OsSPL14* by OsmiR156 defines ideal plant architecture in rice. *Nature Genet.* **42,** 541–544 (2010).
10. Lu, Z. *et al.* Genome-wide binding analysis of the transcription activator IDEAL PLANT ARCHITECTURE1 reveals a complex network regulating rice plant architecture. *Plant Cell* **25,** 3743–3759 (2013).
11. Miura, K. *et al.* OsSPL14 promotes panicle branching and higher grain productivity in rice. *Nature Genet.* **42,** 545–549 (2010).
12. Zhang, Y.-C. *et al.* Overexpression of microRNA OsmiR397 improves rice yield by increasing grain size and promoting panicle branching. *Nature Biotech.* **31,** 848–852 (2013).
13. Yoshida, A. *et al.* TAWAWA1, a regulator of rice inflorescence architecture, functions through the suppression of meristem phase transition. *Proc. Natl Acad. Sci. USA* **110,** 767–772 (2012).
14. Yoshida, A., Ohmori, Y., Kitano, H., Taguchi-Shiobara, F. & Hirano, H.-Y. Aberrant spikelet and panicle1, encoding a TOPLESS-related transcriptional co-repressor, is involved in the regulation of meristem fate in rice. *Plant J.* **70,** 327–339 (2012).
15. Ikeda, K., Ito, M., Nagasawa, N., Kyozuka, J. & Nagato, Y. Rice ABERRANT PANICLE ORGANIZATION 1, encoding an F-box protein, regulates meristem fate. *Plant J.* **51,** 1030–1040 (2007).
16. Oikawa, T. & Kyozuka, J. Two-step regulation of LAX PANICLE1 protein accumulation in axillary meristem formation in rice. *Plant Cell* **21,** 1095–1108 (2009).
17. Bazin, J. *et al.* MiR396 affects mycorrhization and root meristem activity in the legume *Medicago truncatula*. *Plant J.* **74,** 920–934 (2013).
18. Rodriguez, R. E. *et al.* Control of cell proliferation in *Arabidopsis thaliana* by microRNA miR396. *Development* **137,** 103–112 (2010).
19. Liu, H. *et al.* OsmiR396d-regulated OsGRFs function in floral organogenesis in rice through binding to their targets OsJMJ706 and OsCR4. *Plant Physiol.* **165,** 160–174 (2014).
20. Debernardi, J. M., Rodriguez, R. E., Mecchia, M. A. & Palatnik, J. F. Functional specialization of the plant miR396 regulatory network through distinct microRNA–target interactions. *PLoS Genet.* **8,** e1002419 (2012).
21. Kyozuka, J., Tokunaga, H. & Yoshida, A. Control of grass inflorescence form by the fine-tuning of meristem phase change. *Curr. Opin. Plant Biol.* **17,** 110–115 (2014).
22. Feng, J., Liu, T., Qin, B., Zhang, Y. & Liu, X. S. Identifying ChIP-seq enrichment using MACS. *Nat. Protoc.* **7,** 1728–1740 (2012).
23. Gao, X. *et al.* The SEPALLATA-like gene *OsMADS34* is required for rice inflorescence and spikelet development. *Plant Physiol.* **153,** 728–740 (2010).
24. Huang da, W., Sherman, B. T. & Lempicki, R. A. Systematic and integrative analysis of large gene lists using DAVID bioinformatics resources. *Nature Protoc.* **4,** 44–57 (2009).
25. Peer, W. A. From perception to attenuation: auxin signalling and responses. *Curr. Opin. Plant Biol.* **16,** 561–568 (2013).
26. Gallavotti, A. *et al.* Sparse inflorescence1 encodes a monocot-specific *YUCCA-like* gene required for vegetative and reproductive development in maize. *Proc. Natl Acad. Sci.* **105,** 15196–15201 (2008).
27. Tanaka, W., Pautler, M., Jackson, D. & Hirano, H.-Y. Grass meristems II: inflorescence architecture, flower development and meristem fate. *Plant Cell Physiol.* **54,** 313–324 (2013).
28. Zhang, D. & Yuan, Z. Molecular control of grass inflorescence development. *Annu. Rev. Plant Biol.* **65,** 553–578 (2014).
29. Barazesh, S. & McSteen, P. Hormonal control of grass inflorescence development. *Trends Plant Sci.* **13,** 656–662 (2008).
30. Gallavotti, A. The role of auxin in shaping shoot architecture. *J. Exp. Bot.* **64,** 2593–2608 (2013).
31. Yamamoto, Y., Kamiya, N., Morinaka, Y., Matsuoka, M. & Sazuka, T. Auxin biosynthesis by the *YUCCA* genes in rice. *Plant Physiol.* **143,** 1362–1371 (2007).
32. Nelissen, H. *et al.* Dynamic changes in ANGUSTIFOLIA3 complex composition reveal a growth regulatory mechanism in the maize leaf. *Plant Cell* **27,** 1605–1619 (2015).
33. Kim, J. H. & Tsukaya, H. Regulation of plant growth and development by the GROWTH-REGULATING FACTOR and GRF-INTERACTING FACTOR duo. *J. Exp. Bot.* **66,** 6093–6107 (2015).
34. Karimi, M., Inzé, D. & Depicker, A. GATEWAY™ vectors for Agrobacterium-mediated plant transformation. *Trends Plant Sci.* **7,** 193–195 (2002).
35. Franco-Zorrilla, J. M. *et al.* Target mimicry provides a new mechanism for regulation of microRNA activity. *Nature Genet.* **39,** 1033–1037 (2007).
36. Hiei, Y., Ohta, S., Komari, T. & Kumashiro, T. Efficient transformation of rice (*Oryza sativa* L.) mediated by Agrobacterium and sequence analysis of the boundaries of the T-DNA. *Plant J.* **6,** 271–282 (1994).
37. Javelle, M. & Timmermans, M. C. P. *In situ* localization of small RNAs in plants by using LNA probes. *Nature Protoc.* **7,** 533–541 (2012).
38. Ouyang, S. *et al.* The TIGR Rice Genome Annotation Resource: improvements and new features. *Nucleic Acids Res.* **35,** D883–D887 (2007).
39. Saleh, A., Alvarez-Venegas, R. & Avramova, Z. An efficient chromatin immunoprecipitation (ChIP) protocol for studying histone modifications in *Arabidopsis* plants. *Nature Protoc.* **3,** 1018–1025 (2008).
40. Langmead, B., Trapnell, C., Pop, M. & Salzberg, S. L. Ultrafast and memory-efficient alignment of short DNA sequences to the human genome. *Genome Biol.* **10,** R25 (2009).
41. Zhang, Y. *et al.* Model-based Analysis of ChIP-Seq (MACS). *Genome Biol.* **9,** R137 (2008).
42. Bailey, T. L. DREME: motif discovery in transcription factor ChIP-seq data. *Bioinformatics* **27,** 1653–1659 (2011).
43. Wang, K. *et al.* Using FAM labeled DNA oligos to do RNA electrophoretic mobility shift assay. *Mol. Biol. Rep.* **37,** 2871–2875 (2010).
44. Hellman, L. M. & Fried, M. G. Electrophoretic mobility shift assay (EMSA) for detecting protein-nucleic acid interactions. *Nature Protoc.* **2,** 1849–1861 (2007).
45. Chen, W. *et al.* A novel integrated method for large-scale detection, identification, and quantification of widely targeted metabolites: application in the study of rice metabolomics. *Mol. Plant* **6,** 1769–1780 (2013).

Acknowledgements

This research was partly supported by the National Transgenic Research and Development Program (2011ZX08001-004), the 863 Program (2012AA10A303) and the National Science Foundation (31370363) of China. We would like to thank Xuefeng Chen, Yan Zhou, Bo Zhong and Jing Yao (College of Life Science, Wuhan University) for their critical reading and advice during the preparation of this report. We also thank Yu Zhou and Pinji Lei (College of Life Science, Wuhan University) for providing assistance in the bioinformatic analysis.

Author contributions

F.G. performed *in situ* hybridization, SEM, EMSA and phenotypic observation. K.W. conducted microArray, CHIP-seq and RNA-seq analysis. Y.L. performed promoter analysis. Y.C. performed overexpression genesis. P.C. performed qPCR and developed the GRF transgene. Z.S. conducted the construction of the MIM396 vector. J.L. performed hormone analysis. D.J. performed gel blotting of miRNA in the hybrids. F.F. and Y.Z. designed and performed the field experiments. S.L. designed the experiments and wrote the paper.

Additional information

Supplementary information is available online. Reprints and permissions information is available online at www.nature.com/reprints. Correspondence and requests for materials should be addressed to S.L.

Competing interests

The authors declare no competing financial interests.